UC San Diego

UC San Diego Previously Published Works

Title

Senp1 drives hypoxia-induced polycythemia via GATA1 and Bcl-xL in subjects with Monge's disease.

Permalink

https://escholarship.org/uc/item/2pn7w96s

Journal

The Journal of experimental medicine, 213(12)

ISSN

0022-1007

Authors

Azad, Priti
Zhao, Huiwen W
Cabrales, Pedro J
et al.

Publication Date

2016-11-01

DOI

10.1084/jem.20151920

Peer reviewed

eScholarship.org Powered by the California Digital Library
University of California

Senp1 drives hypoxia-induced polycythemia via GATA1 and Bcl-xL in subjects with Monge's disease

Priti Azad,[1] Huiwen W. Zhao,[1] Pedro J. Cabrales,[2] Roy Ronen,[3] Dan Zhou,[1] Orit Poulsen,[1] Otto Appenzeller,[6] Yu Hsin Hsiao,[1] Vineet Bafna,[4] and Gabriel G. Haddad[1,5,7]

[1]Division of Respiratory Medicine, Department of Pediatrics, [2]Department of Bioengineering, [3]Bioinformatics and Systems Biology Graduate Program, [4]Department of Computer Science and Engineering, and [5]Department of Neurosciences, University of California, San Diego, La Jolla, CA 92093
[6]Department of Neurology, New Mexico Health Enhancement and Marathon Clinics Research Foundation, Albuquerque, NM 87122
[7]Rady Children's Hospital, San Diego, CA 92123

In this study, because excessive polycythemia is a predominant trait in some high-altitude dwellers (chronic mountain sickness [CMS] or Monge's disease) but not others living at the same altitude in the Andes, we took advantage of this human experiment of nature and used a combination of induced pluripotent stem cell technology, genomics, and molecular biology in this unique population to understand the molecular basis for hypoxia-induced excessive polycythemia. As compared with sea-level controls and non-CMS subjects who responded to hypoxia by increasing their RBCs modestly or not at all, respectively, CMS cells increased theirs remarkably (up to 60-fold). Although there was a switch from fetal to adult HgbA0 in all populations and a concomitant shift in oxygen binding, we found that CMS cells matured faster and had a higher efficiency and proliferative potential than non-CMS cells. We also established that SENP1 plays a critical role in the differential erythropoietic response of CMS and non-CMS subjects: we can convert the CMS phenotype into that of non-CMS and vice versa by altering *SENP1* levels. We also demonstrated that GATA1 is an essential downstream target of SENP1 and that the differential expression and response of GATA1 and Bcl-xL are a key mechanism underlying CMS pathology.

The Journal of Experimental Medicine

INTRODUCTION

Chronic mountain sickness (CMS) or Monge's disease occurs in up to 20% of individuals residing at high altitude in various regions of the world (León-Velarde et al., 2000; Mejía et al., 2005; Wu, 2005; Jiang et al., 2014). Three large high-altitude populations (Andeans, Ethiopians, and Tibetans) have been extensively studied (Beall, 2000, 2006; Zhou et al., 2013; Udpa et al., 2014), and these have provided a unique opportunity to investigate the mechanisms of adaptation to high-altitude hypoxia and evolution because these human populations have been under selection pressure for centuries (Beall, 2000, 2006; Zhou et al., 2013; Udpa et al., 2014). For Tibetans, *EGLN1*, *EPAS1*, and *PPARα* have seemingly been under positive selection as illustrated in multiple studies (Simonson et al., 2010; Xiang et al., 2013; Lorenzo et al., 2014; Luo et al., 2014). In the Andean population, several studies, including our own, have pointed out that there are several candidate genes, such as *ANP32D*, *SENP1*, *G allele NOS3*, and *vascular endothelial growth factor* (*VEGF*) loci, that likely play a role (Appenzeller et al., 2006; León-Velarde and Mejía, 2008; Zhou et al., 2013). In Ethiopian highlanders, *CBARA1*, *VAV3*, *ARNT2*, and *THRB*, *CIC*, *LIPE*, and *PAFAHIB3* have been linked to adaptation (Alkorta-Aranburu et al., 2012; Scheinfeldt et al., 2012; Udpa et al., 2014; Gonzales and Chaupis, 2015). It is important to note that some of these DNA-selected regions and candidate genes, as in our previous studies (Zhou et al., 2013; Udpa et al., 2014), have been shown to be causally related to the phenotype of tolerance to high-altitude hypoxia. Furthermore, hypoxia-inducible factor (*HIF*) can certainly play an important role in hypoxia adaptation as has been shown by several investigators (Ronen et al., 2014). Such studies demonstrate the complex and multilocus adaptation to hypoxia and indicate that different populations might adapt by using different mechanisms or routes (Ronen et al., 2014). Besides these genotypic differences among these three populations, there exist differences also in terms of phenotypic adaptive responses, such as resting ventilation, hypoxic ventilatory response, oxygen saturation, and hemoglobin concentration (Beall, 2006).

Excessive polycythemia is one of the critical aspects of Monge's disease (Monge et al., 1965; Monge-C et al., 1992). Although it can be argued that polycythemia in CMS subjects could be advantageous at high altitude because an increase in hemoglobin increases O_2-carrying capacity theoretically, this adaptive trait has deleterious effects because blood increases its viscosity, which, in turn, induces serious morbidities such

Correspondence to Gabriel G. Haddad: ghaddad@ucsd.edu

Abbreviations used: BFU-e, erythroid burst-forming unit; CMS, chronic mountain sickness; EB, embryoid body; EPO, erythropoietin; HIF, hypoxia-inducible factor; IP, immunoprecipitation; iPSC, induced pluripotent stem cell; SCF, stem cell factor; SNP, single-nucleotide polymorphism; SUMO, small ubiquitin-like modifier; TPO, thrombopoietin; VEGF, vascular endothelial growth factor.

© 2016 Azad et al. This article is distributed under the terms of an Attribution–Noncommercial–Share Alike–No Mirror Sites license for the first six months after the publication date (see http://www.rupress.org/terms). After six months it is available under a Creative Commons License (Attribution–Noncommercial–Share Alike 3.0 Unported license, as described at http://creativecommons.org/licenses/by-nc-sa/3.0/).

The Rockefeller University Press $30.00
J. Exp. Med. 2016 Vol. 213 No. 12 2729–2744
https://doi.org/10.1084/jem.20151920

as myocardial infarction and stroke (DeFilippis and Aaberg, 2003; Jansen and Basnyat, 2011). This is often the case in these subjects, in addition to pulmonary hypertension, right heart hypertrophy, and ultimately cardiac failure (Penaloza and Arias-Stella, 2007; Naeije, 2010; Naeije and Vanderpool, 2013). The only and inadequate treatment for these patients is periodic phlebotomy.

The high heritability for hemoglobin concentration in the Andean population suggests that it is under natural selection (Beall, 2006). Although erythropoietin (EPO) is considered to be a major regulator of RBC production, the role of EPO in excessive erythropoiesis, particularly in the Andes, is so far inconclusive (León-Velarde et al., 1991; Franke et al., 2013; Haase, 2013). For example, studies in Peru and Bolivia (La Paz) have shown that some residents develop excessive polycythemia despite having similar serum EPO values at the same elevation of healthy highlanders (Dainiak et al., 1989; León-Velarde et al., 1991). These studies would suggest that EPO most likely continues to play a critical role in erythropoiesis at high altitude, and hence, further studies are required to understand its interaction with other genetic loci, which leads to excessive polycythemia. Furthermore, genetic approaches did not reveal any evidence of an association between *EPO* or *EPOR* gene polymorphisms and polycythemia (Mejía et al., 2005). This suggested to us that there must be other possible mechanisms that play an important role in excessive erythropoiesis in high-altitude Andean polycythemia. One major reason for our interest in this extreme phenotype is that we hypothesize that the molecular mechanisms that are underlying this phenotype may teach us about other related diseases at sea level or about protection of tissues when they are hypoxic or ischemic, as we have recently shown from studies at high altitude (Stobdan et al., 2015).

RESULTS

Generation of human induced pluripotent stem cells (iPSCs) from CMS and non-CMS subjects followed by in vitro erythroid differentiation

To understand the genetic basis of CMS, we acquired blood samples as well as skin biopsies from the same individuals (CMS and non-CMS) residing in Peru (~4338 m; corresponding to ~59% of O_2 at sea level). We sequenced the whole genomes from 20 subjects (10 individuals with CMS and non-CMS) and reported on these in a previous study (Zhou et al., 2013). We have now reprogrammed fibroblasts and generated human iPSCs from five CMS and four non-CMS subjects (Table 1), as well as from three sea-level subjects used as controls. The iPSCs were characterized using DNA fingerprinting, high-resolution karyotyping, and alkaline phosphatase staining, as well as assessing the expression of multilineage differentiation markers, as described in detail in the Characterization of iPSCs section of Materials and methods as well as in our previous work (Zhao et al., 2015). DNA fingerprinting analysis confirmed that the iPSC lines were identical to parental fibroblast lines. The reprogramming of iPSCs was confirmed by staining for pluripotency markers and alkaline phosphatase and the ability to differentiate into three germ layers in vitro (Zhao et al., 2015). The expression of transgenes in the mRNA of iPSCs was low or undetectable, and stem array confirmed that the karyotypes of iPSC colonies were normal (Zhao et al., 2015).

We transformed iPSC lines into erythroid cells (refer to the Erythroid induction and differentiation section of Materials and methods) by adopting a previously published protocol (Kobari et al., 2012). We used sequential cytokines mixtures for induction and maturation of erythroid population, as previously described (Fig. 1 A; Kobari et al., 2012). A quantitative assessment was performed of surface markers such as CD34, CD45 (leukocyte common antigen), CD71 (transferrin receptor protein 1), CD36, and CD235a (glycophorin A). Fig. 1 B shows the CD profile under normoxic conditions, including the gradual increase of CD71 and its subsequent fall and the increase in CD235a with time. Sturgeon et al. (2014) have shown that primitive hematopoietic progenitors are KDR (kinase insert domain receptor)$^+$CD235a$^+$, but we believe that CD235a represents erythroid lineage in our studies because their appearance is late in maturation, and this correlates with the timing of hemoglobinization. At earlier stages, CD34 and CD45 increase and then decrease, as expected. The protocol is ~8 wk long for differentiation and maturation of RBCs, and after 8 wk, all populations show ~99.9% are CD235a-positive cells (Fig. 1, A and B). These CD patterns were observed under normoxia in all three populations as shown in Fig. 1 B, Fig. 2, and Fig. 3 A. To determine the effect of hypoxia, we altered this procedure by exposing cells either to hypoxia or normoxia at the embryoid body (EB) stage and studied the differences among CMS and non-CMS cells (Fig. 2).

Replicating the disease in the dish: Marked differences between CMS and non-CMS cells in response to hypoxia

To emulate high-altitude hypoxia, we exposed cells to 5% O_2 (Fig. 2) for 3 wk at the EB stage (after 1 wk in normoxia, as described in the legend of Fig. 1). We measured the response of the cells to hypoxia on day 28 by FACS using CD235a as an erythroid marker. Fig. 2 shows a remarkable difference in response to hypoxia among the three different groups. On the one hand, sea-level subjects increased the relative proportion of CD235a cells modestly, as expected (by ~7%), whereas the non-CMS group did not respond to hypoxia at all with a relative proportion of ~0.5% CD235a cells. On the other hand, CMS subjects had a marked response, increasing to ~57%, corresponding to a huge increase of many folds (Fig. 2). Fig. 2 (A and B) shows the robust response of each of the CMS (n = 5), non-CMS (n = 4), and sea-level (n = 3) subjects (***, $P < 0.001$; one-way ANOVA with Tukey posthoc analysis). Furthermore, to determine interclonal variability, we have now tested three clones for each of the three subjects in each group under hypoxia (Fig. 2 C). The interclonal variability among the clones for each group is not significant as determined by

Table 1. **Summary of non-CMS and CMS subjects from Cerro de Pasco used in the current study as well as their medical test scores**

Group	Subject no.	Age	Dizziness	Physical weakness	Mental fatigue	Anorexia	Muscle weakness	Joint pain	Breathlessness	Palpitations	Disturbed sleep	Cyanosis	Injected conjunctive	Dilation	Paresthesia	Headache	Tinnitus	Hct score	Sat score	Hct	Sat (%)	CMS score
CMS	N-1	22	0	0	0	0	0	0	2	2	2	2	2	0	2	3	3	3	0	65	85	21
	N-2	37	0	0	0	1	0	1	2	0	0	2	2	0	2	3	0	3	3	76	80	19
	N-3	34	0	0	1	0	1	0	0	0	2	2	0	0	2	3	3	3	0	63	83	17
	N-4	34	0	1	1	0	0	1	2	2	0	2	2	2	0	3	0	3	3	65	84	22
	N-5	43	0	1	1	0	0	1	2	2	2	2	2	2	0	3	3	3	3	80	71	27
non-CMS	N-1	33	1	0	0	0		0	0	0	2	2	0	2	0	0	0	0	0	51	85	7
	N-2	31	0	0	0	0	0	0	0	0	0	0	0	0	0	0	0	0	0	54	90	0
	N-3	23	0	0	0	0	0	0	0	0	0	0	0	0	0	3	0	0	0	52	90	3
	N-4	31	0	0	0	0	0	0	0	0	0	0	0	0	0	0	0	0	0	54	84	0

Note the major differences in hematocrit (Hct), O_2 saturation (Sat), and CMS scores between the two subject populations.

one-way ANOVA (P = 0.99; Fig. 2 C). The variability among the clones for each subject was 5–10%, whereas the smallest difference between the groups was 5–10-fold. In addition, we also used the pooling method of Chou et al. (2015) (n = 20–25 clones) for each of the groups: CMS, non-CMS, and sea level (Chou et al., 2015). As expected, we also observed that the erythropoietic response of CMS under hypoxia is remarkably and significantly higher than both the non-CMS and sea-level control groups (relative proportion of CD235a being on average 72 ± 13.7 in CMS cells and 0.78 ± 0.2 in non-CMS cells; not depicted). Hence, we conclude that the polycythemic response of CMS is genetic in nature, and clonal variability is minimal as compared with the robust phenotype.

This in vitro experiment replicated the high-altitude in vivo response of the three populations. In addition, we have now used footprint-free Sendai technology and retroviral vectors to generate iPSCs. With these Sendai-generated iPSCs, we observed a similar pattern of phenotypic differences in hypoxia: an exuberant response in CMS and a blunted one in non-CMS cells (Fig. 2 A). These results in our subject-specific iPSC lines strongly suggest a genetic basis of the polycythemia in the Andean population. To build a dose response and because there was such a large response to 5% O_2 in CMS cells, we elected to expose cells to other levels of hypoxia (10% and 1.5%). Fig. 2 D shows the differential sensitivity of the three populations to graded hypoxia, with a huge sensitivity to hypoxia in cells from CMS subjects.

We next defined the functional and maturational characteristics of the erythroid lineage in the three populations by performing (a) assessment of surface markers and membrane proteins, (b) colony-forming potential, (c) efficiency of differentiation, (d) hemoglobin pattern, and (e) oxygen-binding affinity. Under normoxia, CD profiles (CD45, CD71, and CD235a) at each week were not statistically significantly different between the groups (sea level, non-CMS, and CMS; Fig. 3 A). However, we observed dramatic differences in the maturational CD profile when we compared CMS and non-CMS cells in hypoxia (Fig. 3 B and Table 2). After 3 wk of hypoxic exposure, the relative proportion of $CD235a^+$ cells was 50–60% in CMS cells, whereas this proportion was <5% of cells in non-CMS subjects (Fig. 3 B). CMS cells also produced significantly higher number of erythroid burst-forming units (BFU-Es; fourfold) as compared with non-CMS cells (Fig. 3 C), suggesting that the erythroid progenitors in the CMS population have a higher proliferative potential than the non-CMS population. Table 2 shows the amplification potential for all three groups: although all groups had similar rates of erythroid production in normoxia, CMS cells produced a higher proportion of EBs as well as erythroid cells in hypoxia (Table 2). Our results indicate that hypoxia affects both proliferation as well as maturation of CMS cells (but not the other populations), as we observed differences in both the number of cells as EBs and BFU-Es as well as changes in CD markers. By performing hemoglobin analysis, we also observed a switch from fetal to adult HgbA0 starting at week

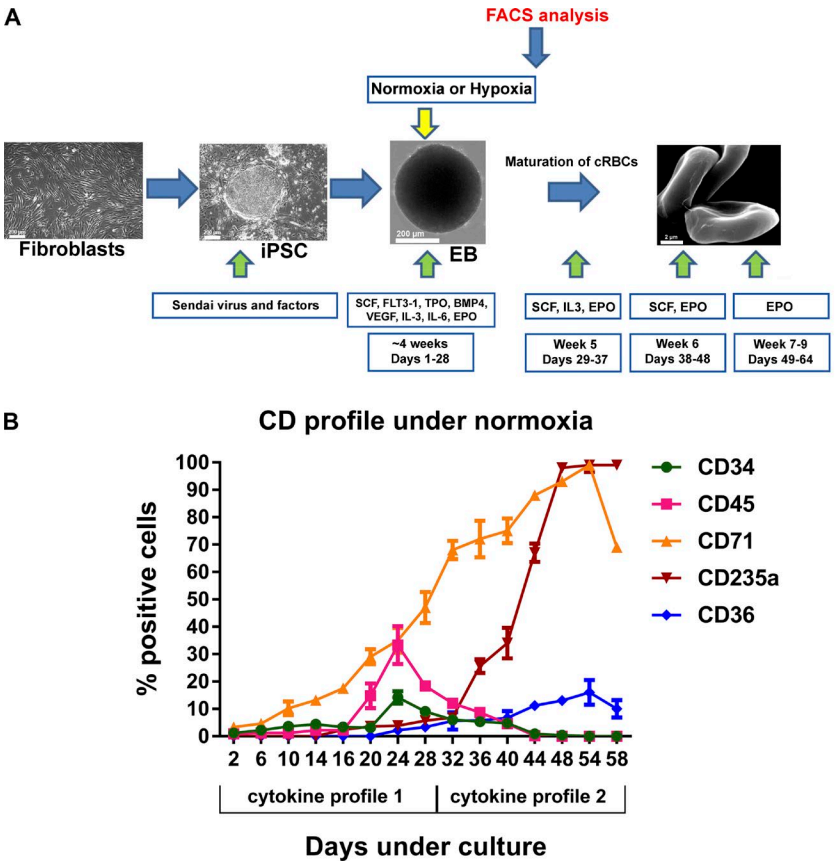

Figure 1. **Production of erythroid cells from human iPSC.** (A) Schematic representation of the successive culture steps for production of cultured RBCs (cRBCs) from fibroblasts. Fibroblasts were transformed to iPSCs using the Yamanaka factors. Clumps of undifferentiated iPSCs were cultured in erythroid body (EB) medium for 28 d in the presence of a mixture of cytokines (cytokine profile 1). After 1 wk of culturing in normoxia, erythroid bodies were allowed to differentiate for 3 wk in normoxia/hypoxia, and the populations were analyzed by flow cytometry at day 28 or were allowed to mature further under cytokine profile 2 by sequential sets of cocktails and analyzed at day 58. Bars: (fibroblasts) 200 µm; (iPSC) 200 µm; (EB) 200 µm; (red blood cell, right) 2 µm. (B) CD analysis of various CD markers (CD34, CD45, CD36, CD71, and CD235a) under normoxia for sea-level samples. Each experiment was done in three replicates, and the experiment was done at least three times. The cells are cultured as erythroid bodies in cytokine profile 1 and as single cells in cytokine profile 2 (sequential mixture of cytokines). Error bars represent the mean ± SEM of at least two to three measurements. The experiment was repeated at least three times.

6 of differentiation of iPSCs (Fig. 3, D and F). Indeed, there was an increase in the proportion of adult HgbA0 (an increase in α and β globin expression) and a decrease in expression of ε and γ (Fig. 3 F). Concomitantly, there was a shift in P50 from 14 mmHg to 22 mmHg (Fig. 3 D), consistent with maturation of RBC function in vivo. Furthermore, during erythroid maturation, band3 (HCO3-Cl transporter) and Glut1 appeared in all cell populations (Fig. 3 E).

Based on our previous findings of whole-genome sequencing of CMS and non-CMS subjects, we then studied the role of one of the candidate genes that we mined from our detailed analysis (Zhou et al., 2013). In addition, we performed a reduction experiment to investigate the role of various known cytokines presumed to be essential for erythropoiesis to probe at potential pathways involved in RBC formation in each of the three populations (refer to the Reduction experiment for cytokines [SCF, TPO, FLT3, BMP4, VEGF, IL3, IL6, and EPO] section of Materials and methods).

Critical role of SENP1 in polycythemia

SENP1 is a small ubiquitin-like modifier (SUMO) protease that cleaves SUMO groups off of several targets, including GATA1 and HIF1 (Cheng et al., 2007). Fig. 4 A shows 66 single-nucleotide polymorphisms (SNPs) identified as significantly divergent in allele frequency between CMS and non-CMS individuals (differential SNPs). Three of these differential SNPs (SNP accession nos. rs74910025, rs12581972, and rs726354) are in the cluster of ENCODE (The Encyclopedia of DNA Elements) transcription factor–binding sites (ENCODE Project Consortium, 2012; Rosenbloom et al., 2012). This site (chr12:48500334; rs726354) also overlaps a DNase I–hypersensitive region observed mainly in blood cells (Sabo et al., 2004). Furthermore, they also overlap with different regulatory regions: chr12:48500334 (rs726354) overlaps with the promoter site, chr12:48478354 (rs12581972) overlaps with one of the CTCF sites, and chr12:48472343 (rs74910025) overlaps with one of the enhancer sites (Fig. 4 A). It is interesting to note that the differential SNP rs726354 coincides with binding sites of transcriptional factors such as E2F1, POLR2A, GABPA, TAF1, ELF1, and GATA1. Another independent study from the Andean cohorts from Cerro de Pasco consisting of 84 CMS cases and 91 healthy controls reproduced and validated our previous results for divergent SNPs in the *SENP1* region (Cole et al., 2014). We therefore hypothesized that the differential SNPs in the regulatory regions alter the expression of *SENP1* in CMS or non-CMS subjects. Indeed, when we compared the transcriptional response of CMS to that of non-CMS cells in hypoxia, we found that CMS cells up-regulated SENP1, suggesting that this up-regulation could underlie the excessive erythrocytosis present in the CMS population (Zhou et al., 2013). We have indeed observed a significant increase not only in *SENP1* mRNA, but also at the protein level in

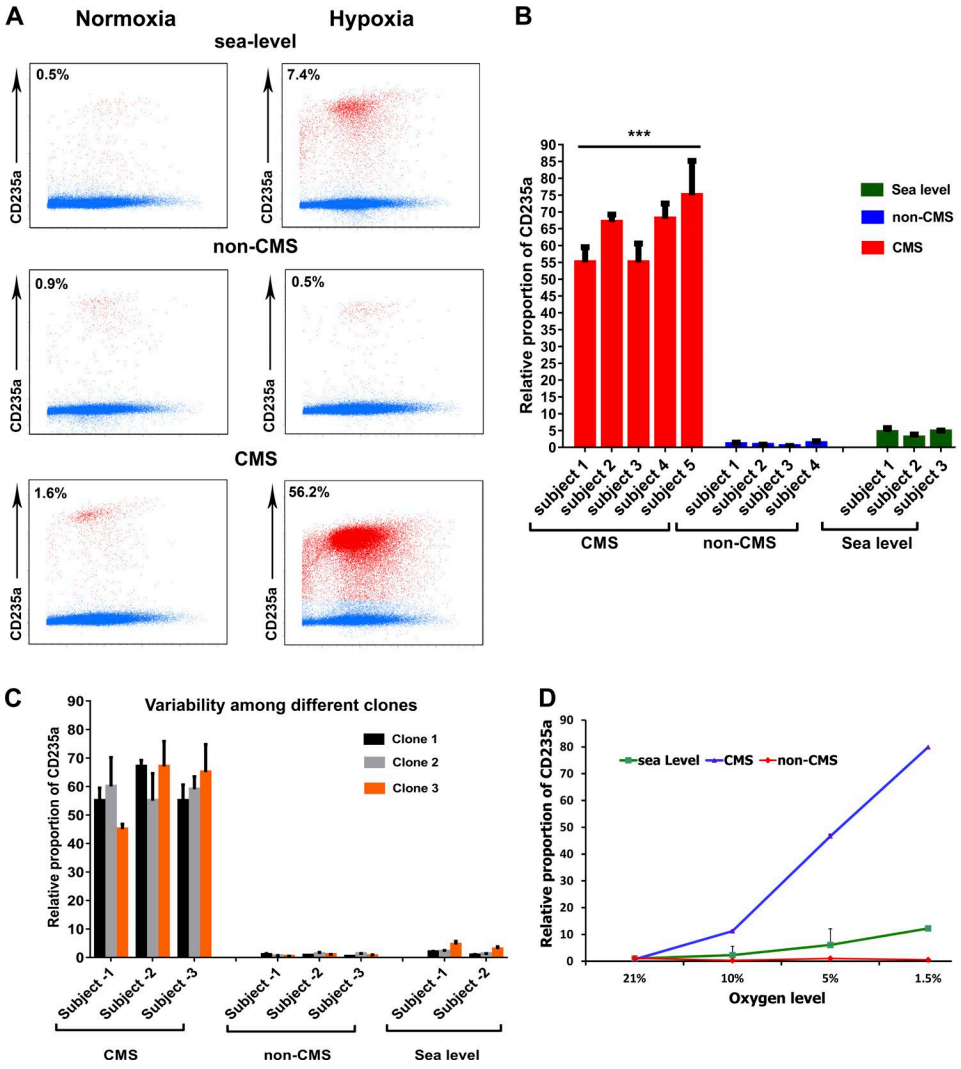

Figure 2. **Hypoxic response of sea-level, non-CMS, and CMS cells: Marked response of CMS samples.** (A) Flow cytometric analysis using CD235a (glycophorin A) as a marker after culturing as detailed in Fig. 1 at the EB stage at day 28. Sendai virus results: Representative FACS plots of sea level, non-CMS, and CMS in normoxia (left) and in hypoxia (right). The dot plot represents the live cells as gated through propidium iodide. $CD235a^+$ cells are shown in red along the y axis, and $CD235a^-$ cells are shown in blue. The percentage in each figure represents the relative proportion of CD235a cells. There are major differences between CMS (bottom) versus the non-CMS (middle) and sea-level (top) samples. The FACS plots are representative of one experiment. Similar results were obtained in all the experimental repeats. (B) Summary of hypoxic response of CMS patients (n = 5 subjects) and non-CMS (n = 4 subjects) and sea-level (n = 3 subjects) control subjects. The graph depicts the relative proportion of CD235a quantified 3 wk after the administration of hypoxia (5% O_2). There is a significantly striking difference between sea level, non-CMS, and CMS under hypoxia. ***, $P < 0.001$. Error bars represent the mean ± SEM of at least two to three measurements. The experiment was repeated at least three times. (C) Summary of interclonal variability among the subjects: three clones (clones 1, 2, and 3) were tested for three subjects (subjects 1, 2, and 3) for each group: CMS, non-CMS, and sea level. The y axis depicts the relative proportion of CD235a under hypoxia for different clones. Error bars represent the mean ± SEM of at least two to three measurements. (D) Dose response. The graph represents the response (as measured by proportion of CD235a [y-axis]) of CMS, non-CMS, and sea-level cells to 21%, 10%, 5%, and 1.5% O_2 levels (x axis). Each point depicts the mean ± SEM of at least two to three measurements. CMS shows hyperresponsiveness at 10, 5, and 1.5% O_2. The experiment was repeated at least three times.

CMS subjects under hypoxia ($P < 0.05$; Fig. 4 B). This notion is strengthened by previous studies demonstrating that SENP1 regulates erythropoiesis and that *SENP1*$^{-/-}$ mouse embryos die of anemia (Yu et al., 2010).

To determine whether SENP1 plays an important role in the exuberant response to hypoxia in CMS subjects, we generated a lentiviral vector to down-regulate SENP1in CMS iPSCs. There was a significant reduction of *SENP1* in the shRNAi-generated clones at both the mRNA and protein levels (Fig. 4, C and D). With *SENP1* shRNAi, the relative proportion of CD235a fell remarkably to <1%, as compared with a mean (n = 3) of ~60% observed in noninfected CMS

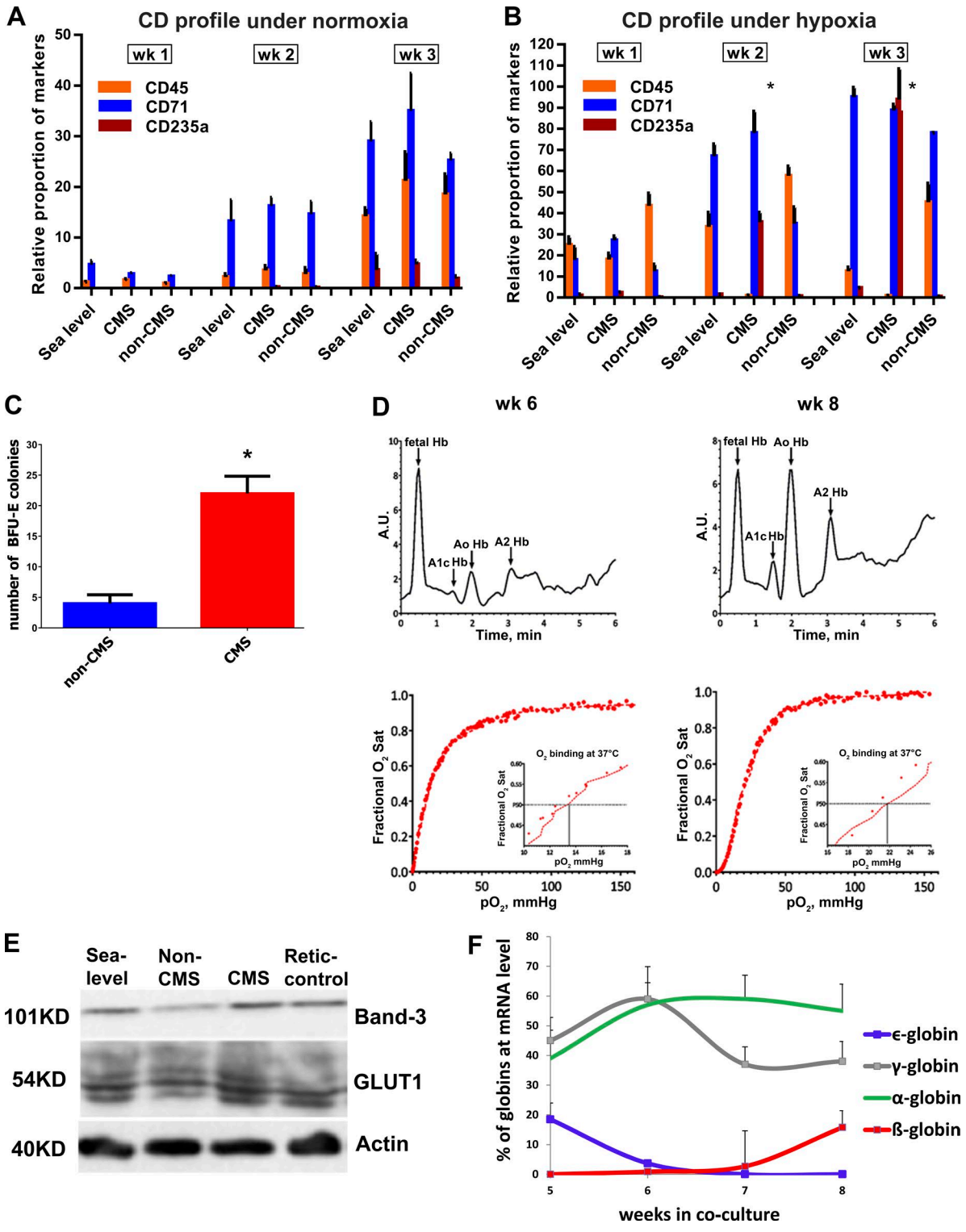

Figure 3. **Characterization of the erythroid cells under normoxia and hypoxia.** (A) CD analysis of various markers (CD45, CD71, and CD235a) for all populations under normoxia (21% O_2). The cells are cultured as described in Fig. 1. Note that the CD profiles are similar for all groups under normoxia. (B) CD analysis of various markers (CD45, CD71, and CD235a) for all populations under hypoxia (5% O_2). The cells were cultured as described in Fig. 1. During week 3, we see significant differences in the proportion of CD235a between CMS and the controls (sea level and non-CMS). (A and B) Each experiment was done in three replicates, and experiments were repeated at least three times. (C) BFU-e assay under hypoxia (5% O_2). The y axis represents the number of BFU-e colonies. The experiment was done in three replicates and repeated twice. (D) Hemoglobin (Hb) analyses and function of erythroid cells with high-

lines (Fig. 4 E). Multiple clones of *SENP1* knock-out showed a similar loss of phenotype (Fig. 4 E), affirming the critical role of *SENP1* in the increased sensitivity of CMS to hypoxia. We also overexpressed *SENP1* cDNA in the non-CMS iPSC lines (Fig. 4 F), and interestingly, the non-CMS cells (with overexpressed *SENP1*) show a similar polycythemic phenotype as the CMS cells (Fig. 4, F and G). Hence, by manipulating *SENP1*, we converted the CMS polycythemic trait into a non-CMS blunted response and vice versa. This proves our hypothesis that SENP1 plays a fundamental role in the CMS polycythemia of high altitude and the lack of this phenotype in the non-CMS population.

GATA1 and Bcl-xL are differentially expressed in CMS and non-CMS cell lines

To further explore the underlying molecular mechanisms of the polycythemic phenotype in CMS subjects, we performed a cytokine reduction experiment in which we removed one of the eight cytokines and kept the rest (the other seven) intact during the process of differentiating iPSCs. We found that removal of stem cell factor (SCF), BMP4, IL3, IL6, and Epo one at a time adversely affected the formation of RBCs in all three cell populations (Table 3), indicating that an exogenous source was important for their development. However, removal of thrombopoietin (TPO), FLT3L, and VEGF from the medium of CMS cells did not change the marked erythropoietic response, unlike the sea-level and non-CMS cells, which were very affected, resulting in a nil response to hypoxia in these two populations of subjects. We then hypothesized that either (a) CMS cells produce these factors (e.g., TPO) to compensate for those that are removed or (b) there is potentially a cross-talk between pathways that bypasses the need for these specific factors in CMS, unlike in the other two populations. Actually, our real-time PCR data showed that CMS subjects produce significantly higher *VEGF* (but not *TPO* or *FLT3*) in hypoxia (Fig. 5 A), with no change in VEGF, TPO, or FLT3 receptors. To determine whether there is a cross-talk between VEGF, TPO, and Flt3 signaling pathways, we tested the expression of downstream factors, such as *GATA1*, *Bcl-xL*, and *STAT5 a,b*. In fact, CMS cells produced significantly higher levels of *Bcl-xL* in hypoxia (Fig. 5 A) and copious amounts (>10-fold) of GATA1, as compared with the other cell populations (Fig. 5 A). This is also the case for CMS cells producing significantly higher GATA1 protein when compared with non-CMS cells (Fig. 5, A and B). These results became very informative because SENP1 stabilizes GATA1 and leads to its up-regulation as well as the up-regulation of GATA1-responsive genes, e.g., *Bcl-xL*. Hence, we performed these experiments in CMS and non-CMS at the mRNA and protein levels. CMS cells produced significantly higher levels of GATA1-inducible genes *Slc4a1* and *Alas2* than non-CMS cells (Fig. 5, C and D). In contrast, we observed higher expression of GATA1-repressive genes *cMyc* and *cKit* in non-CMS cells (Fig. 5, C and E).

SENP1-mediated GATA1 activation is essential for polycythemic response of CMS

SENP1-mediated desumoylation is considered to be a regulatory mechanism for the activation of transcription factors such as GATA1. When we tested the sumoylation levels of GATA1 in both CMS and non-CMS cells (EBs), we found that non-CMS had much higher levels of sumoylated GATA1 as compared with CMS patients in hypoxia (Fig. 5 F). The relatively high levels of sumoylation of target genes under hypoxia is in accordance with a previous study by Jiang et al. (2015), where they observed higher levels of sumoylated HIF under hypoxia. We verified our finding by immunoprecipitation (IP) experiments and observed significantly higher levels of GATA1 sumoylation in non-CMS samples as compared with CMS samples under hypoxia (Fig. 6, A and B). The SUMO-GATA1/GATA1 ratios are significantly different between CMS and non-CMS cells under hypoxia (Fig. 6 B; $P < 0.01$). These ratios are within the range of published mouse *SENP1KO* studies (Yu et al., 2010). To prove that increased hypoxia sensitivity of CMS cells is linked to SENP1-desumoylation GATA1 activation, we designed a fused SUMO-GATA1 construct using SUMO-fusion technology. The reason for using this construct was to determine whether this fused SUMO-GATA1 cannot be desumoylated by SENP1 and, hence, to directly test the function of SENP1 in the desumoylation and activation of GATA1. The overexpression of fused SUMO-GATA1 in GATA1 knock-out background did not induce the CMS phenotype in hypoxia, suggesting that SENP1 is critical in activating GATA1 and the erythropoietic response under hypoxia (Fig. 6 C). It is important to note that the fused SUMO-GATA1 has reduced activity as measured by *EPOR* and *cMyc* levels (e.g., mean *EPOR* mRNA levels as measured by real-time PCR are 0.155 for CMS cells and 0.11 for CMS cells containing fused SUMO-GATA1 construct; not depicted), but even with this level of reduced activity, GATA1 does not reestablish the CMS phenotype under hypoxia. However, when we overexpressed GATA1-K137R (which cannot be sumoylated) in GATA1 knock-out

performance liquid chromatography profiles of erythroid cells at weeks 6 and 8. Note a shift in hemoglobin from fetal to adult A0. The O2-binding curve also shows a transition of P50 from 14 mmHg (week 6) to 22 mmHg (week 8). Shown is one representative image of data points at weeks 6 and 8. The experiment was repeated at least five times. A.U., arbitrary units; Sat, saturation. (E) Western blot of RBCs (erythroblasts). Note the presence of BAND-3 and GLUT1 in all lanes (normalized to actin). Retic, reticulocytes used as controls. (F) Globin expression by quantitative PCR for sea level and globin switching in time in culture. Similar trends were observed during maturation for all groups. $n = 3$ and error bars represent SD. Globin percentage is calculated as described by Qiu et al. (2008). The experiment was repeated at least three times. *, $P < 0.05$.

background, we observed that both CMS and non-CMS showed an increased polycythemic response under hypoxia (Fig. 6 E). We verified the overexpression of the fused SUMO-GATA1 and GATAK137R-mutant constructs by Western blotting (Fig. 6, D and F). Further, by overexpressing the GATA1 target gene *Bcl-xL*, we only partially rescued the blunted response to hypoxia in non-CMS (Fig. 7, A and B). The non-CMS *Bcl-xL* overexpression line had significantly higher erythropoietic response than uninfected non-CMS ($P < 0.05$), but it was as much as the CMS line. The overexpression of *Bcl-xL* partially increased the proliferation capacity of erythroid progenitors in non-CMS as shown in Fig. 7 C. Collectively then, our data show that SENP1 activates GATA1 and downstream signaling pathways.

DISCUSSION

Based on our previous work (Zhou et al., 2013) detailing the whole-genome analysis of high-altitude dwellers in the Andes, we had hypothesized that several candidate genes played a role in the extreme phenotype of polycythemia of CMS subjects. Taken differently, these potential candidates could have played an important role in blunting the response of non-CMS subjects to high-altitude hypoxia and, hence, in allowing these subjects to better adapt to high altitude. In fact, one question that arises from both our previous study (Zhou et al., 2013) and our current one is whether the non-CMS subjects have adapted by a loss of function of *SENP1* (or potentially also other genes). It is at present a hypothesis, and we do not have any such proof except that an up-regulation of *SENP1* in hypoxia leads to the phenotype and its down-regulation to an absence of polycythemia. Another question that can be asked is the cause of the up-regulation of *SENP1* during hypoxia in CMS subjects. Although this can be thought of as potentially an epigenetic phenomenon because it is linked to hypoxia exposure, it is not part of the scope of this work. Indeed, we have focused in this study on genetic mechanisms that are responsible for polycythemia, namely the response to *SENP1* and its targets, particularly *GATA1* and *Bcl-xL*, by both cell populations.

There were several reasons for choosing *SENP1* (as a candidate gene) to understand the phenotype in CMS and non-CMS populations. First, we have previously shown that the expression of this gene is increased with hypoxia in CMS but not in non-CMS (Zhou et al., 2013); second, down-regulating its orthologue in flies dramatically enhances survival rates under hypoxia (Zhou et al., 2013); third, a null *senp1* mutation in mice leads to embryonic lethality caused by anemia in mice (Yu et al., 2010); and finally, it has several desumoylation targets and hence may affect several genes, transcription factors, and pathways (Cheng et al., 2007). Herein, our work shows that SENP1 is central to erythropoiesis during hypoxia: an increase in SENP1 increases remarkably the ability of non-CMS to form RBCs, and a down-regulation of SENP1 almost totally eliminates the exuberant response of the CMS to form RBCs during hypoxia. One could argue that because SENP1 has potentially many desumoylation targets, it might not be surprising for SENP1 to have such a dramatic effect on response to hypoxia. However, to have only one gene, albeit a transcription factor (e.g., GATA1), resulting (Fig. 6) in such a huge effect in eliminating erythropoiesis when desumoylated by SENP1 is clearly remarkable. On the one hand, it would not appear unreasonable to suspect that HIF would be involved in erythropoiesis in CMS subjects because SENP1 stabilizes HIF1α (Cheng et al., 2007) which regulates EPO expression and level. On the other hand, EPO, a downstream effector of HIF, has not been shown to be much different when CMS and non-CMS were compared (Dainiak et al., 1989; León-Velarde et al., 1991). In addition, we did not observe any significant difference in *EPOR* levels between the CMS and non-CMS in our in vitro model (*EPOR* mRNA levels as measured by real-time PCR normalized by *GAPDH*: CMS is 0.155 ± 0.001 and non-CMS is 0.157 ± 0.001). Actually, by adding the same concentration of EPO in the media of the iPSCs of both cell populations, we removed in essence the effect of EPO in our phenotype. However, our current studies do not eliminate the effect of EPO in CMS subjects in vivo. Indeed, EPO is an essential mediator of erythropoiesis, and hence, further investigation is required to confirm its role in CMS (Villafuerte et al., 2014).

Conceptually, the reprogramming of fibroblasts into iPSCs and differentiation of these into RBCs is novel, especially when used for understanding high altitude–induced polycythemia using very unique and valuable populations that have adapted (or maladapted) to hypoxia for thousands of years (CMS vs. non-CMS populations). Our previous finding that *SENP1* is a major candidate gene found in a selective DNA sweep in the Andean population was very

Table 2. **Efficiency of differentiation of RBCs under normoxia and hypoxia**

Efficiency	Sea level	CMS	Non-CMS
Normoxia			
No. of EB cells/10^6 stem cells	1.08 ± (0.075)	0.92 ± (0.028)	1.19 (0.036)
No. of erythroid cells/10^6 stem cells	230 ± (0.16)	190 ± (0.2)	210 ± (0.16)
Hypoxia (5% O_2)			
No. of EB cells/10^6 stem cells	1.5 ± (0.68)	2.6 ± (0.28)	1.4 ± (0.036)
No. of erythroid cells/10^6 stem cells	270 ± (0.1)	310 ± (0.25)	166 ± (0.23)

The numbers in parenthesis represent SE. SE is for six experiments for each group. All values are 10^6 times.

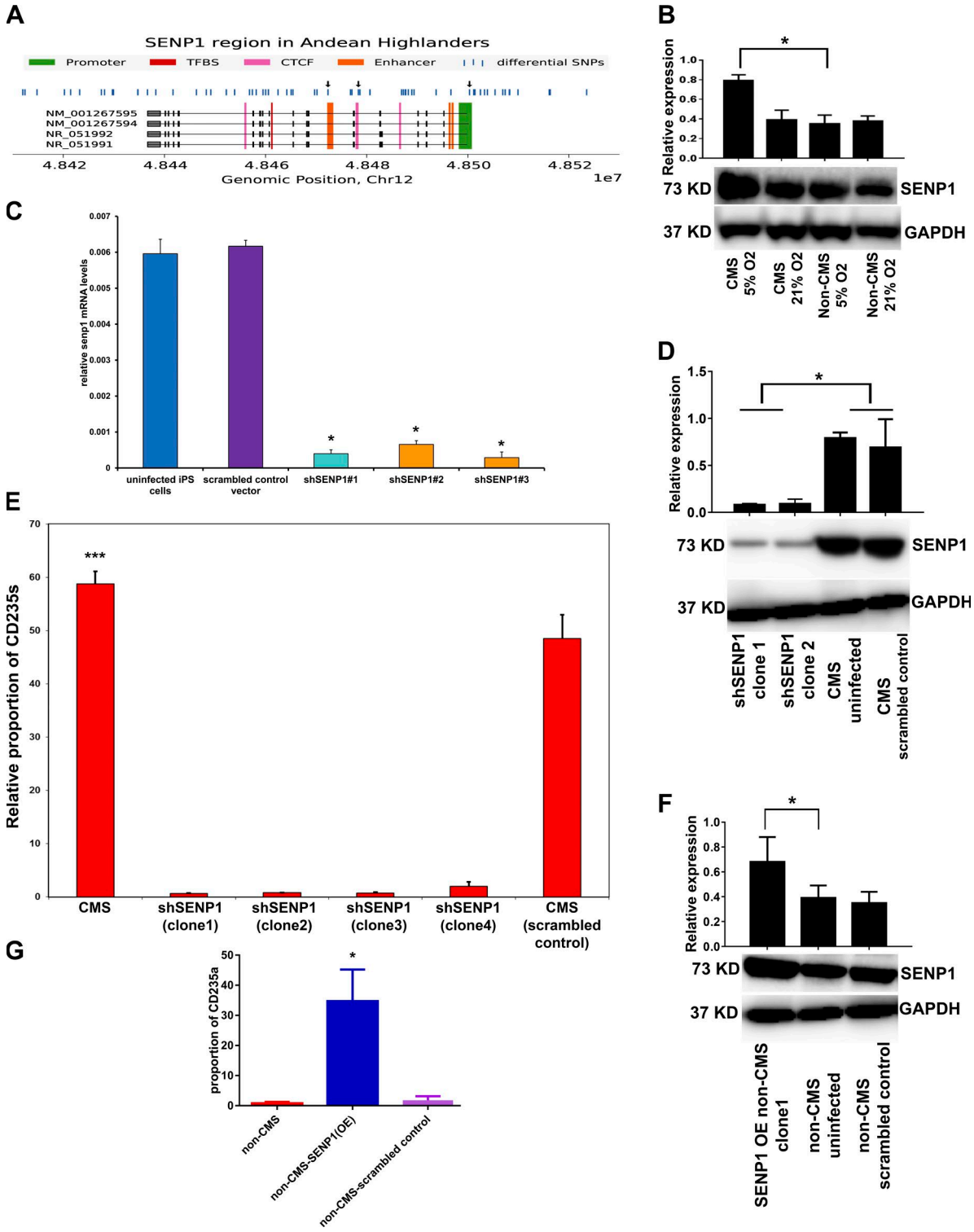

Figure 4. **Role of SENP1 in CMS polycythemia in the Andean population.** (A) The *SENP1* region in Andean highlanders. Four known transcripts of human SENP1 with accession nos. (NCBI RefSeq) are shown. Note that SENP1 is transcribed from the negative strand (i.e., right to left). Overlaid above in blue are the genomic positions of 66 SNPs deemed differential by Zhou et al. (2013). Three of our differential SNPs (marked with black arrows) overlap with different regulatory regions such as promoters and enhancers, as described in the Critical role of SENP1 in polycythemia section of Results. These SNPs show a strong signal of frequency differentiation between the non-CMS and CMS highlanders, indicative of strong positive selection in the region. (B) Western blot analysis of SENP1 protein expression under hypoxia (5% O_2) and normoxia (21% O_2) for CMS and non-CMS groups. The representative blot

interesting. However, it is important to note that it is difficult to determine which of the 66 structural variants found to be differential between the populations is the casual variant. By using the haplotype allele frequency score (which some of us previously developed; Ronen et al., 2015), we could separate the carriers of the favored mutations from the noncarriers. From this haplotype allele frequency analysis, it is reasonable to conclude that the non-CMS carry a favorable mutation that decreases their predisposition to increase erythropoiesis under hypoxia as in the CMS subjects. In this study, we confirmed the critical role of SENP1 and showed the role of specific targets in erythropoiesis in the CMS/non-CMS populations.

Although there have been studies in cell lines that suggested that SENP1 regulates GATA1 (Yu et al., 2010), our study is the first to directly link Monge's disease to GATA1 activation through SENP1. That hypoxia-induced polycythemia of CMS subjects is not dependent on cytokines such as TPO and FLT3 is intriguing and new, especially that the non-CMS and sea-level subjects have a different response, indicating the involvement of different pathways for erythropoiesis in these populations. Our study opens a new avenue to study EPO-independent pathways linked to growth factors involved in erythropoiesis in humans.

Another possible mechanism for the differences seen among the CMS and non-CMS subjects is related to apoptosis and proliferation that could also be linked to SENP1 regulation (Xu et al., 2015). Indeed, we see significant differences in the expression of the antiapoptotic gene *Bcl-xL* between CMS and non-CMS subjects. By overexpressing *Bcl-xL* in non-CMS cells, we can partially rescue the phenotype and make them comparable to sea-level individuals.

In conclusion, our study has shown that the excessive polycythemic response in CMS subjects is an oligogenic trait and can be modeled in vitro using cutting-edge techniques. Functionally, we have established that SENP1 plays a critical role in the differential erythropoietic response of CMS and non-CMS subjects based on our genetic studies whereby knock-down or overexpression of *SENP1* can convert the CMS phenotype into that of non-CMS and vice versa. The reduction experiments as well as the sumoylation differences in the GATA1 and fused SUMO-GATA1 experiments strongly suggest that GATA1 is downstream of target of SENP1 and is involved in the polycythemia of this Andean population. Furthermore, decreased expression of the antiapoptotic gene *Bcl-xL* (GATA1 downstream effector) in the non-CMS cells is responsible in part for the blunted erythropoietic response under hypoxia particularly at the erythroid progenitor stage. We believe that the utility of this iPSC-derived hypoxia model of the Andean population that has lived in chronic hypoxia over thousands of years lies not only in the understanding of hypoxia-induced polycythemia, but also in other hypoxia-driven diseases experienced at sea level, as we have recently shown for the Ethiopian population (Stobdan et al., 2015).

MATERIAL AND METHODS

Subjects and clinical characterization

All subjects were adult males residing in the Andean mountain range in Cerro de Pasco, Peru at an elevation of ∼4,338 m. Sea-level controls were adult individuals of similar age group who lived at sea level their entire life and have normal hematocrit and oxygen saturation. CMS patients fulfilled the diagnostic criteria for CMS, or Monge's disease, based on their hematocrit, O_2 saturation, and CMS score (>12). Each subject signed an informed written consent under protocols approved by the University of California, San Diego and the Universidad Peruana Cayetano Heredia.

Preparation of dermal fibroblasts from human skin biopsies

3-mm skin punch biopsy samples were obtained from male highlanders with CMS (n = 5) and without CMS (n = 4) in Cerro de Pasco, Peru, as well sea-level individuals (n = 3). The skin biopsies were mechanically dissociated and plated for dermal fibroblast expansion in DMEM supplement with 10% fetal calf serum, 2.5% penicillin/streptomycin, and 1% fungizone antibiotic (Invitrogen). Fibroblasts grew from explants after 2–3 wk and were passaged when they achieved 80% confluence.

is shown is from one experiment. The relative levels were computed for n = 5 for CMS and n = 4 for non-CMS under hypoxia and normoxia. Data represent at least two to three measurements. The experiment was repeated at least twice for each subject. (C) iPSCs were infected with lentivirus and selected by puromycin. shSENP1#1, shSENP1#2, and shSENP1#3 represent the three clones selected. Each clone showed significant down-regulation of Senp1 expression by quantitative PCR, compared with uninfected iPSCs, as well as an iPSC line infected by control vector. Data represent two measurements in duplicate. (D) Western blot analysis of the loss of SENP1 expression in the shRNA clones. Lanes 1 and 2 show significant reduction in SENP1 levels in shRNA clones 1 and 2 as compared with uninfected and scrambled controls. Each bar represents the mean ± SEM of at least two to three measurements. The experiment was repeated at least two times for each subject. (E) Loss of vigorous erythropoietic response of CMS cells to hypoxia. The first bar represents the response of CMS cells to hypoxia. CMS-Senp1-shRNA represents the CMS cells that were infected by shRNA of Senp1 using lentivirus infection. Four different clones were tested for each line. Data represent three measurements in triplicates. The experiment was repeated three times. An unpaired Student's t test was used. (F) Overexpression of SENP1 in non-CMS iPSCs. The blot shows a representative image for one experiment. We observed a twofold increase in expression in non-CMS in the cDNA overexpression cell line. Data represent three measurements in triplicates. The experiment was repeated twice. An unpaired Student's t test was used. (G) SENP1 overexpression (OE) leads to marked increase in RBCs in non-CMS erythroid cell differentiation. The scrambled control overexpression did not change the phenotype of CMS. Each bar represents the mean for each clone measured in triplicates. The experiment was repeated three times. Error bars represent the mean ± SEM. *, $P < 0.05$; ***, $P < 0.001$.

Table 3. **Reduction experiment eliminating one cytokine at a time from the cytokines added to the cells**

Factor reduction (—)	CMS	Non-CMS	Sea level
SCF	0.2	0	0
TPO	31.1	0	0.1
Flt3	31.5	0	0
BMP4	0.1	0.1	0
VEGF	68.8	0	0
IL-3	2.3	0.1	0.6
IL-6	1.4	0.1	0.2
Epo	0.1	0	0.1

Relative proportion of CD235a marker after 3 wk under hypoxia eliminating one factor at a time. Eliminated cytokines are shown in column 1 for each experiment. The numbers under each population represent relative percentages of CD235a. The relative levels of CD235a in all populations with all factors in the media range in CMS (36–91.6%), non-CMS (0.2–1%), and sea level (3.1%–9.1%) are shown. Example: When TPO is eliminated in culture, 31.1% of cells (for CMS) were CD235a positive; for non-CMS and sea level, it was nil. Hence, CMS cells do not need TPO but sea-level and non-CMS cells do.

Reprogramming of human fibroblast cells and generation of iPSCs

Retroviral vectors containing the Yamanaka factors (OCT4, cMYC, KLF4, and SOX2 human cDNAs) were manufactured by Salk Institute Gene Transfer, Targeting, and Therapeutics Core. We have switched now to footprint-free Sendai virus technology. Nonintegrated iPSCs are generated using SeV vectors encoding OCT3/4, SOX2, KLF4, and cMYC (CytoTune-iPS 2.0 Sendai Reprogramming kit) following the manufacturer's protocol. In brief, infected fibroblast cells were cultured using a feeder-free method with Essential 8 medium. Compact colonies containing iPSC colonies appeared after 3 wk and were mechanically picked, transferred to a Matrigel-coated dish (BD), and expanded in mTeSR medium (STEMCELL Technologies; Zhao et al., 2015). Three clones were picked from each subject and were analyzed to assess the interclone variability.

Characterization of iPSCs

3 wk after transduction, compact iPSC colonies appeared. These were similar to human embryonic stem cells and were characterized by large nuclei and scant cytoplasm. The colonies were manually picked and cultured on the Matrigel-coated plates for expansion. Three clones were collected from each individual subject. DNA was extracted from fibroblasts and iPSC lines using a DNase blood and tissue kit (QIAGEN) for the subsequent analysis. DNA-fingerprinting analysis and stem array, a high-resolution karyotyping, were performed by Cell Line Genetics. DNA-fingerprinting analysis confirmed that the obtained iPSC line was identical to parental somatic cell lines. Furthermore, all iPSC colonies had a normal karyotype (Zhao et al., 2015). To validate complete reprogramming, the following evidence was included: (a) positive staining for NANOG and tumor-related antigen–1-81, (b) positive staining for alkaline phosphatase, (c) similar expression of prominent endogenous pluripotency genes such as OCT4, SOX2, cMYC, KLF4, NANOG, and LIN28 was observed in iPSCs and H9 cells, (d) in vitro EB-mediated differentiation with expression of multilineage differentiation markers including ectodermal markers (microtubule-associated protein 2 [MAP2] and paired box 6 [PAX6]), mesodermal markers (Msh homeobox 1 [MSX1] and α smooth muscle actin [α-SMA]), and endodermal markers (cytokeratin 8 [CK8] and CK18), and (e) the presence of exogenous reprograming factors in the genomic DNA of iPSCs but the expression of transgenes in the mRNA of iPSCs was low or undetectable (Zhao et al., 2015). These data suggested that iPSCs were pluripotent and have the ability to differentiate into three germ layers in vitro.

Erythroid induction and differentiation

Human iPSC passages 9–20 were grown in Matrigel (BD)-coated dishes supplemented with mTeSR media (STEMCELL Technologies). The protocol for erythroid induction was adapted from a study by Kobari et al. (2012). For all subjects, the cultures were started with approximately 10^7 cells. Human iPSCs were differentiated by formation of EBs (hEB) during 27 d in a liquid culture medium on the basis of IMDM (Biochrom), 450 μg/ml holo human transferrin (Sigma-Aldrich), 10 μm g/ml recombinant human insulin (Roche), 2 IU/ml heparin, and 5% human plasma in the presence of 100 ng/ml SCF, 100 ng/ml TPO, 100 ng/ml FLT3 ligand, 10 ng/ml rhu bone morphogenetic protein 4 (BMP4), 5 ng/ml rhu VEGF (VEGF-A165), 5 ng/ml IL-3, 5 ng/ml IL-6 (PeproTech), and 3 U/ml Epo. Terminal differentiation was achieved by further culturing in sequential combination of cytokines as described by Kobari et al. (2012)

Hypoxia treatment

EBs were cultured for 1 wk at 37°C in 5% CO_2 in air. After 1 wk, the EBs were transferred to a hypoxic incubator set at 37°C, 5% O_2, and 5% CO_2 for 3 wk. FACS analysis was done at day 28 at the EB stage. For the dose response experiment, 1.5%, 5%, and 10% O_2 levels were used.

BFU-e and CFU-e assay

FACS-sorted $CD34^+$ cells were plated at a density of 10^5 cells per 35-mm dish combined with MethoCult H4034 Optimum media and 2% FBS. Dishes were incubated at 37°C in an incubator with 5% CO_2 and 5% O_2 for 14 d, at which time colonies were scored for BFU-E and CFU–GEMM (granulocyte, erythrocyte, monocyte, megakaryocyte).

Flow cytometric analysis

EBs were dissociated using Accuatase Cell Dissociation reagent (Invitrogen), washed with PBS supplemented with 2% FBS, and filtered through a 70-μm cell strainer (Falcon; BD). Cells were treated with propidium iodide (Sigma-Aldrich) before analysis. Cells were stained with hCD45 (leukocyte common antigen), hCD71 (transferrin receptor protein 1), and hCD235a-PE (glycophorin A) from BD and analyzed by a FACSCanto cell analyzer (BD) using FACSDiva software (version 6.0; BD).

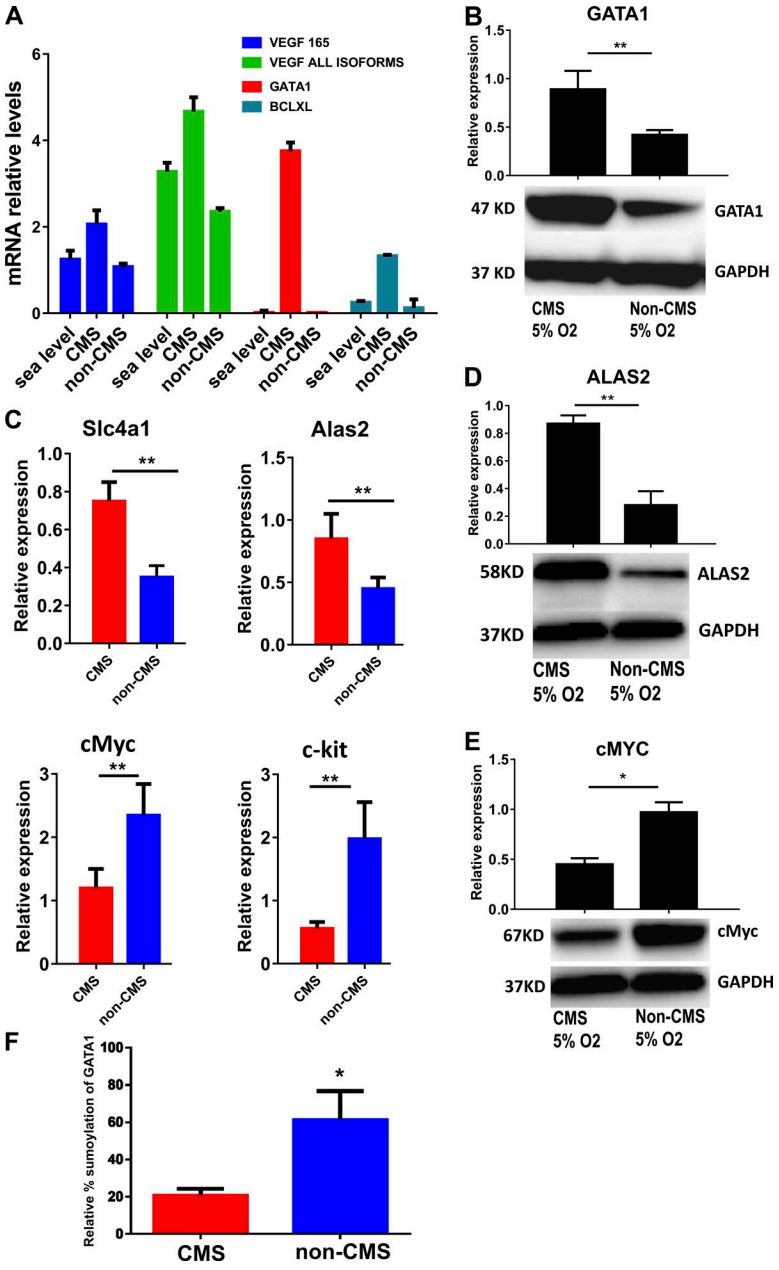

Figure 5. **Significant difference in expression between CMS versus non-CMS and sea-level cells.** (A) Relative VEGF, GATA1, and Bcl-xL expression by quantitative PCR (normalized with GADPH) in cultures grown in hypoxia in media. CMS cells produced significantly higher levels of VEGF, GATA1, and Bcl-xL. (B) Western blot analysis of GATA1 protein levels. The figure shows a representative blot for one experiment. The bars shows the relative levels for $n = 4$ for each group (CMS and non-CMS). The experiment was repeated at least three times. An unpaired Student's t test was performed. (C) Relative mRNA levels of GATA1-inducible (Scl4a and Alas2) and repressive (cMyc and cKit) genes for CMS and non-CMS subjects. (D) Western blot analysis of Alas2 protein levels. The figure shows a representative blot for one experiment. (E) Western blot analysis of cMyc protein levels. The figure shows a representative blot for one experiment. (C–E) The bars show the relative levels for $n = 4$ for each group (CMS and non-CMS). The experiment was repeated at least three times. An unpaired Student's t test was performed. (F) Non-CMS cells show significantly high amount of sumoylated GATA1 as compared with CMS and sea-level controls. $P < 0.05$; unpaired Student's t test. The results are the summary for $n = 4$ for both CMS and non-CMS groups. Each bar represents the mean, and error bars represent the SE. For each sample, the levels were measured in triplicates. Each experiment was repeated three times. *, $P < 0.05$; **, $P < 0.01$.

Hemoglobin analysis and oxygen-binding assay

Hemoglobin fractions were separated and quantified by ion exchange high-performance liquid chromatography. Oxygen equilibrium curves were obtained by deoxygenating O_2-equilibrated samples in Hemox buffer at 37°C using a Hemox analyzer (TCS Scientific Corp). After thorough deoxygenation under nitrogen, the cell suspensions were equilibrated at different partial pressures of oxygen by slow bubbling 40% oxygen into the cuvette. The fractional saturation was estimated by simulation of the absorption spectra in the visible regions as a linear combination of the fully deoxygenated and oxygenated spectra of the cells suspension. The globin fractions were calculated by real-time PCR using the method described by Qiu et al. (2008).

Sumoylation assay using an ELISA-based kit

Cytosolic and membrane proteins were isolated using standard protein isolation protocols and kits (Abcam). Relative sumoylation levels under hypoxia were measured using an In Vivo Protein Sumoylation Assay Ultra kit (EpiQuik). It is a calorimetric-based measurement, whereby the ratio or intensity of the sumoylation, which is proportional to the conjugated SUMO amount, can be quantified through the signal report–color development system. Anti-GATA1 and anti–SUMO-1 antibodies were purchased from Abcam. The percent sumoylation was measured using the following formula: % Sumoylation = OD (Hypoxia sample − Negative control)/OD (Normoxia sample − Negative control) × 100%.

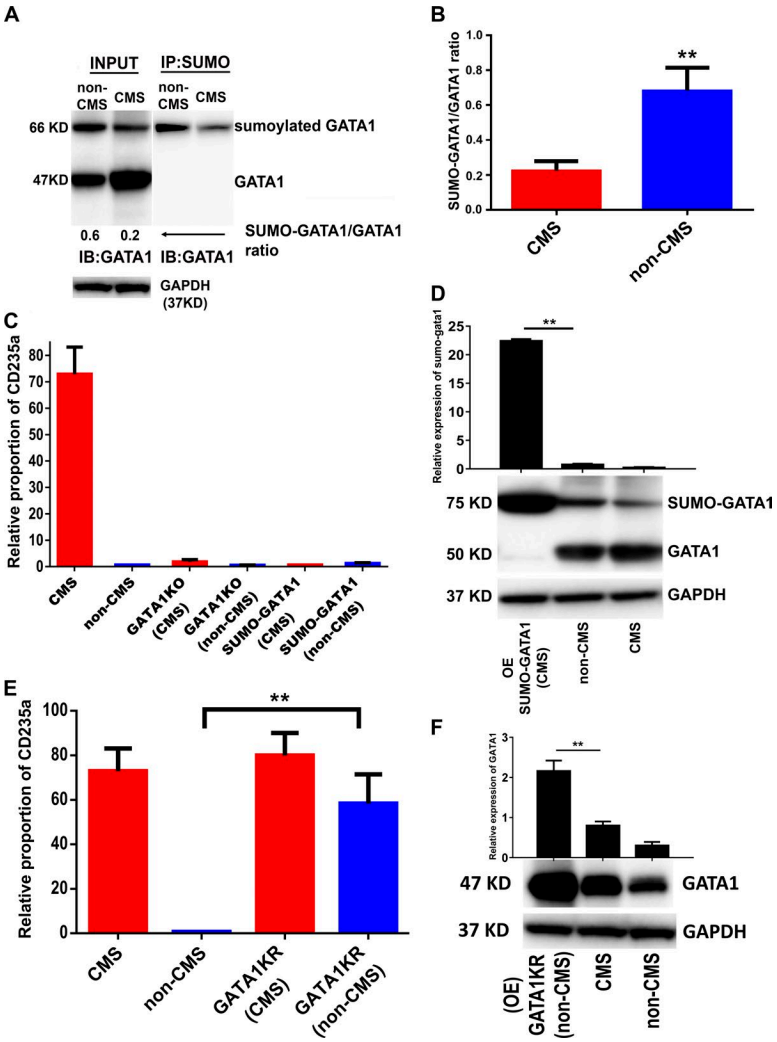

Figure 6. **SENP1 desumoylase activity plays a critical role in GATA1 desumoylation and activation.** (A) A representative blot showing that non-CMS cells show significantly higher levels of sumoylated GATA1. The sumoylated form of GATA1 was determined by IP with anti-SUMO followed by Western blotting with anti-GATA1. The ratios of SUMO-GATA1/GATA1 were quantified. IB, immunoblot. (B) Non-CMS cells show a significantly high SUMO-GATA1/GATA-1 ratio as compared with CMS. $P < 0.05$; Student's *t* test. The results are the summary for $n = 4$ for both CMS and non-CMS groups. Each bar represents the mean, and error bars represent SE. For each sample, the levels were measured in triplicates. Each experiment was repeated three times. (C) Fused SUMO-GATA1 cannot restore the remarkable CMS phenotype in a background of GATA1 KO. Non-CMS had a similar result. Each bar represents a mean of three replicates, and the experiment was repeated at least twice. (D) Western blot analysis confirming significantly higher levels of SUMO-fused Gata1 in the overexpressed (OE) line. Lane 1 represents CMS cells lines overexpressing fused SUMO-GATA1 in the GATA1 KO background. Please note the significantly higher levels of SUMO-GATA1 in the GATA1 KO background. Lane 2 shows the relative levels of SUMO-GATA1 and GATA1 in non-CMS cells. Lane 3 shows the relative levels of SUMO-GATA1 and GATA1 in CMS cells. (E) GATAK137R (GATA1KR) mutant causes the polycythemic phenotype in both CMS and non-CMS subjects under hypoxia. Each bar represents a mean of three replicates, and the experiment has been repeated at least twice. (F) Western blot analysis showing overexpression of GATA1K137R in the non-CMS cells. Lane 1 represents non-CMS cell lines overexpressing GATA1K137R in the GATA1KO background. Lane 2 shows the relative levels GATA1 in uninfected CMS cells. Lane 3 shows the relative levels of GATA1 in uninfected non-CMS cells. (C–F) Each bar represents the mean of three replicates, and the experiment was repeated at least twice. Error bars represent SEM. **, $P < 0.01$.

IP, immunoblotting, and sumoylation ratios

Cytosolic and membrane proteins were isolated using standard protein isolation protocols and kits (Abcam). IP was performed using an IP kit (Thermo Fisher Scientific) following the procedure described by Yu et al. (2010). IP was performed using an anti-SUMO antibody (Abcam) followed by Western blot analysis using anti-GATA1 antibody. Primary antibodies against SENP1, GAPDH, and GATA1 were obtained from Santa Cruz Biotechnology, Inc. Antibodies against BAND3, GLUT1, SUMO1, CMYC, and ALAS were obtained from Abcam. In brief, 20 µg of lysate supernatant were separated by 10% SDS-PAGE and transferred to a nitrocellulose membrane. The blots were developed using enhanced chemilumescent reagents (Bio-Rad Laboratories) and the ChemiDoc XRS+ molecular imager (Bio-Rad Laboratories).

Reduction experiment for cytokines (SCF, TPO, FLT3, BMP4, VEGF, IL3, IL6, and EPO)

EBs were treated with eight different cytokines. Each mixture has one cytokine missing at a time (eight cytokines minus one cytokine). EBs were transferred to hypoxic conditions as described in the Hypoxia treatment section and analyzed after 3 wk by flow cytometry as mentioned in the Flow cytometric analysis section.

Real-time PCR for VEGF, FLT3, and TPO reduction experiments

EBs were extracted from the culture media after weeks 1, 2, and 3 in hypoxia. RNA was isolated from EB using an RNeasy Mini kit (QIAGEN). cDNA was produced from total RNA through RT-PCR using a Superscript III First-Strand Synthesis system (Invitrogen). Real-time PCR was performed using a GeneAmp 7900 sequence detection system using POWER SYBR Green chemistry (Applied Biosystems). The primer sequences were as follows: VEGF165-L, 5′-ATCTTCAAGCCA TCCTGTGTGC-3′; VEGF165-R, 5′-CAAGGCCCACAG GGATTTTC-3′; Vegf-A(all isoforms)F, 5′-GAGATGAGC TTCCTACAGCAC-3′; Vegf-A(all isoforms)R, 5′-TCACCG CCTCGGCTTGTCACAT-3′; FLT3-F, 5′-TTTCACAGG ACTTGGACAGAGATTT-3′; FLT3-R, 5′-GAGTCCGGG TGTATCTGAACTTCT-3′; TPO-F, 5′-CAGGACTGAAAA

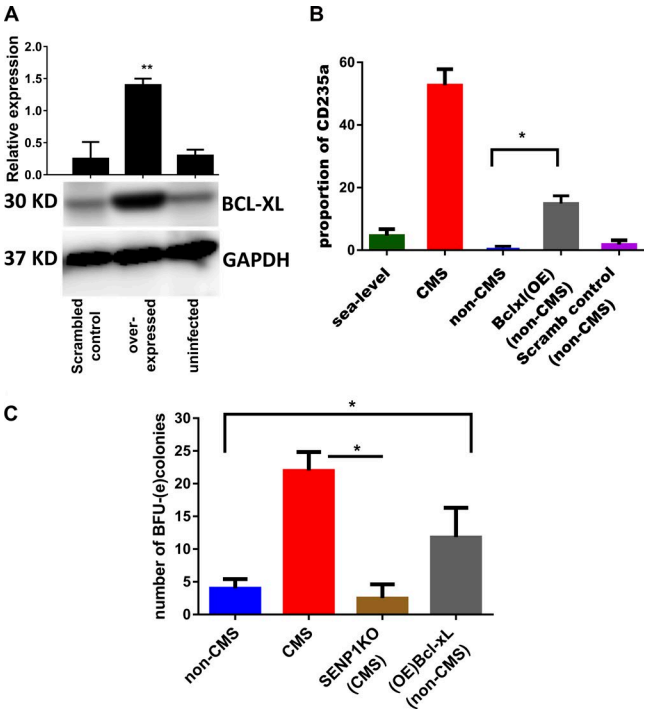

Figure 7. **GATA1 target Bcl-xL plays a role in CMS polycythemia and erythroid progenitors.** (A) Western blot analysis confirming the overexpression of Bcl-xL in the non-CMS levels. Lane 1 represents the non-CMS cell line infected with scrambled control. Lane 2 represents non-CMS cells overexpressing Bcl-xL construct. Lane 3 shows the expression levels on uninfected non-CMS cells. Each bar represents a mean of three replicates, and the experiment was repeated at least twice. Error bars represent SEM. **, $P < 0.01$. (B) Overexpression (OE) of Bcl-xL partially rescues the blunted response of non-CMS cells (gray bar). Error bars represent mean ± SEM. Measurements were done in triplicates. The experiment was repeated three times. The response of scrambled control (pink bar) as well as sea-level (green), CMS (red), and non-CMS (blue) uninfected cells are also shown. *, $P < 0.05$; Student's *t* test. Scramb, scrambled. (C) Overexpression of Bcl-xL increases the number of BFU-e in non-CMS cells (gray). SENP1KO decreases the number of colonies in CMS cells (brown). *, $P < 0.05$; Student's *t* test. Each bar represents the mean, and error bars represent SE. For each sample, the levels were measured in triplicates. Each experiment was repeated three times.

GGGAATCA-3′; TPO-R, 5′-CGTTGGAAGGCCTTG AATTT-3′; GATA1-L, 5′-CCTGCTTTGTTGCCAATG-3′; GATA1-R, 5′-CTGCTCCACTGTTACGGATAC-3′; Bcl-xL-L, 5′-GCAGGTATTGGTGAGTCGGATCGC-3′; and Bcl-xL-R, 5′-CACAAAAGTATCCCAGCCGCCG-3′. The expression level of *GADPH* was used to normalize the results. GADPH-L, 5′-CTGGCATTGCCCTCAACGACC-3′ and GADPH-R, 5′-CTTGCTGGGGCTGGTGGTCC-3′.

Lentiviral vectors and transduction of iPSCs for knock-down of Senp1

The shRNA-SENP1 construct was a gift from G. Salvesen's laboratory (Sanford-Burnham Prebys Medical Discovery Institute, La Jolla, CA). Human *SENP1* and *Bcl-xL* (open reading frame) in an expression-ready lentiviral system construct was purchased from GE Healthcare. The packaging and lentivirus generation was done by Salk Institute Gene Transfer, Targeting, and Therapeutics Core. Transduced cells were selected at 0.5 µg/ml puromycin (Sigma-Aldrich) or blasticidin (EMD Millipore). The expression of SENP1 was confirmed by real-time PCR.

Generation of GATA1 KO and fused SUMO-GATA1 constructs

GATA1 KO construct was generated with blasticidin resistance by Gentarget. The fused SUMO-GATA1 construct was generated by Lifesensors, and the construct was subcloned, and the lentivirus was generated by ViGENE. Transduced cells were selected at 0.5–1 µg/ml blasticidin (EMD Millipore) and 0.5 µg/ml puromycin (Sigma-Aldrich). GATA1K137R construct was a gift from W. Min's (Yale University, New Haven, CT) and C. Santoro's (Interdisciplinary Research Center on Autoimmune Diseases, Novora, Italy) laboratories. This construct was subcloned, and the lentivirus was generated by ViGENE. Transduced cells were selected for 1 µg/ml puromycin (Sigma-Aldrich).

Statistical tests

One-way ANOVA followed by Tukey posthoc analysis was used to test significant differences between the subjects of each group (CMS, non-CMS, and sea level), as well as to assess interclonal variability. Student's *t* tests were performed to evaluate differences between the various groups.

ACKNOWLEDGMENTS

We thank Dr. Kobari (UK), Dennis Young, Ali Akbari, and Dr. S. Shattil (University of California, San Diego) for their technical assistance and advice. Our special thanks to Dr. D. Fasci and Dr. G. Salvesen for senp1 plasmid and Drs. W. Min and C. Santoro for GATA1K137R construct.

This study is funded by National Institutes of Health (NIH) grants (1P01HL098053 and 5P01HD32573) to G.G. Haddad, National Science Foundation grants (NSF-CCF-1115206 and NSF-III-1318386) and NIH grants (5RO1-HG004962 and U54 HL108460) to V. Bafna, and NIH grants (R56HL123015 and R01-HL52684) to P. Cabrales.

The authors declare no competing financial interests.

Submitted: 10 December 2015
Revised: 2 June 2016
Accepted: 6 October 2016

REFERENCES

Alkorta-Aranburu, G., C.M. Beall, D.B. Witonsky, A. Gebremedhin, J.K. Pritchard, and A. Di Rienzo. 2012. The genetic architecture of adaptations to high altitude in Ethiopia. *PLoS Genet.* 8:e1003110. http://dx.doi.org/10.1371/journal.pgen.1003110

Appenzeller, O., T. Minko, C. Qualls, V. Pozharov, J. Gamboa, A. Gamboa, and Y. Wang. 2006. Gene expression, autonomic function and chronic hypoxia:lessons from the Andes. *Clin. Auton. Res.* 16:217–222. http://dx.doi.org/10.1007/s10286-006-0338-3

Beall, C.M. 2000. Tibetan and Andean patterns of adaptation to high-altitude hypoxia. *Hum. Biol.* 72:201–228.

Beall, C.M. 2006. Andean, Tibetan, and Ethiopian patterns of adaptation to high-altitude hypoxia. *Integr. Comp. Biol.* 46:18–24. http://dx.doi.org/10.1093/icb/icj004

Cheng, J., X. Kang, S. Zhang, and E.T.Yeh. 2007. SUMO-specific protease 1 is essential for stabilization of HIF1α during hypoxia. *Cell.* 131:584–595. http://dx.doi.org/10.1016/j.cell.2007.08.045

Chou, B.K., H. Gu, Y. Gao, S.N. Dowey, Y. Wang, J. Shi, Y. Li, Z. Ye, T. Cheng, and L. Cheng. 2015. A facile method to establish human induced pluripotent stem cells from adult blood cells under feeder-free and xeno-free culture conditions: a clinically compliant approach. *Stem Cells Transl. Med.* 4:320–332. http://dx.doi.org/10.5966/sctm.2014-0214

Cole, A.M., N. Petousi, G.L. Cavalleri, and P.A. Robbins. 2014. Genetic variation in SENP1 and ANP32D as predictors of chronic mountain sickness. *High Alt. Med. Biol.* 15:497–499. http://dx.doi.org/10.1089/ham.2014.1036

Dainiak, N., H. Spielvogel, S. Sorba, and L. Cudkowicz. 1989. Erythropoietin and the polycythemia of high-altitude dwellers. *Adv. Exp. Med. Biol.* 271:17–21. http://dx.doi.org/10.1007/978-1-4613-0623-8_3

DeFilippis, A., and S. Aaberg. 2003. Blood is thicker than water: The management of hyperviscosity in adults with cyanotic heart disease. *J. Gen. Intern. Med.*

ENCODE Project Consortium. 2012. An integrated encyclopedia of DNA elements in the human genome. *Nature.* 489:57–74. http://dx.doi.org/10.1038/nature11247

Franke, K., M. Gassmann, and B. Wielockx. 2013. Erythrocytosis: the HIF pathway in control. *Blood.* 122:1122–1128. http://dx.doi.org/10.1182/blood-2013-01-478065

Gonzales, G.F., and D. Chaupis. 2015. Higher androgen bioactivity is associated with excessive erythrocytosis and chronic mountain sickness in Andean Highlanders: a review. *Andrologia.* 47:729–743. http://dx.doi.org/10.1111/and.12359

Haase, V.H. 2013. Regulation of erythropoiesis by hypoxia-inducible factors. *Blood Rev.* 27:41–53. http://dx.doi.org/10.1016/j.blre.2012.12.003

Jansen, G.F., and B. Basnyat. 2011. Brain blood flow in Andean and Himalayan high-altitude populations: evidence of different traits for the same environmental constraint. *J. Cereb. Blood Flow Metab.* 31:706–714. http://dx.doi.org/10.1038/jcbfm.2010.150

Jiang, C., J. Chen, F. Liu, Y. Luo, G. Xu, H.Y. Shen, Y. Gao, and W. Gao. 2014. Chronic mountain sickness in Chinese Han males who migrated to the Qinghai-Tibetan plateau: application and evaluation of diagnostic criteria for chronic mountain sickness. *BMC Public Health.* 14:701. http://dx.doi.org/10.1186/1471-2458-14-701

Jiang, Y., J. Wang, H. Tian, G. Li, H. Zhu, L. Liu, R. Hu, and A. Dai. 2015. Increased SUMO-1 expression in response to hypoxia: Interaction with HIF-1α in hypoxic pulmonary hypertension. *Int. J. Mol. Med.* 36:271–281. http://dx.doi.org/10.3892/ijmm.2015.2209

Kobari, L., F. Yates, N. Oudrhiri, A. Francina, L. Kiger, C. Mazurier, S. Rouzbeh, W. El-Nemer, N. Hebert, M.C. Giarratana, et al. 2012. Human induced pluripotent stem cells can reach complete terminal maturation: in vivo and in vitro evidence in the erythropoietic differentiation model. *Haematologica.* 97:1795–1803. http://dx.doi.org/10.3324/haematol.2011.055566

León-Velarde, F., and O. Mejía. 2008. Gene expression in chronic high altitude diseases. *High Alt. Med. Biol.* 9:130–139. http://dx.doi.org/10.1089/ham.2007.1077

León-Velarde, F., C.C. Monge, A. Vidal, M. Carcagno, M. Criscuolo, and C.E. Bozzini. 1991. Serum immunoreactive erythropoietin in high altitude natives with and without excessive erythrocytosis. *Exp. Hematol.* 19:257–260.

León-Velarde, F., A. Gamboa, J.A. Chuquiza, W.A. Esteba, M. Rivera-Chira, and C.C. Monge. 2000. Hematological parameters in high altitude residents living at 4,355, 4,660, and 5,500 meters above sea level. *High Alt. Med. Biol.* 1:97–104.

Lorenzo, F.R., C. Huff, M. Myllymäki, B. Olenchock, S. Swierczek, T. Tashi, V. Gordeuk, T. Wuren, G. Ri-Li, D.A. McClain, et al. 2014. A genetic mechanism for Tibetan high-altitude adaptation. *Nat. Genet.* 46:951–956. http://dx.doi.org/10.1038/ng.3067

Luo, Y., Y. Wang, H. Lu, and Y. Gao. 2014. 'Ome' on the range: update on high-altitude acclimatization/adaptation and disease. *Mol. Biosyst.* 10:2748–2755. http://dx.doi.org/10.1039/C4MB00119B

Mejía, O.M., J.T. Prchal, F. León-Velarde, A. Hurtado, and D.W. Stockton. 2005. Genetic association analysis of chronic mountain sickness in an Andean high-altitude population. *Haematologica.* 90:13–19.

Monge, C., R. Lozano, and J. Whittembury. 1965. Effect of blood-letting on chronic mountain sickness. *Nature.* 207:770. http://dx.doi.org/10.1038/207770a0

Monge-C, C., A. Arregui, and F. León-Velarde. 1992. Pathophysiology and epidemiology of chronic mountain sickness. *Int. J. Sports Med.* 13:S79–S81. http://dx.doi.org/10.1055/s-2007-1024603

Naeije, R. 2010. Physiological adaptation of the cardiovascular system to high altitude. *Prog. Cardiovasc. Dis.* 52:456–466. http://dx.doi.org/10.1016/j.pcad.2010.03.004

Naeije, R., and R. Vanderpool. 2013. Pulmonary hypertension and chronic mountain sickness. *High Alt. Med. Biol.* 14:117–125. http://dx.doi.org/10.1089/ham.2012.1124

Penaloza, D., and J. Arias-Stella. 2007. The heart and pulmonary circulation at high altitudes: healthy highlanders and chronic mountain sickness. *Circulation.* 115:1132–1146. http://dx.doi.org/10.1161/CIRCULATIONAHA.106.624544

Qiu, C., E.N. Olivier, M. Velho, and E.E. Bouhassira. 2008. Globin switches in yolk sac-like primitive and fetal-like definitive red blood cells produced from human embryonic stem cells. *Blood.* 111:2400–2408. http://dx.doi.org/10.1182/blood-2007-07-102087

Ronen, R., D. Zhou, V. Bafna, and G.G. Haddad. 2014. The genetic basis of chronic mountain sickness. *Physiology (Bethesda).* 29:403–412.

Ronen, R., G. Tesler, A. Akbari, S. Zakov, N.A. Rosenberg, and V. Bafna. 2015. Predicting carriers of ongoing selective sweeps without knowledge of the favored allele. *PLoS Genet.* 11:e1005527. http://dx.doi.org/10.1371/journal.pgen.1005527

Rosenbloom, K.R., T.R. Dreszer, J.C. Long, V.S. Malladi, C.A. Sloan, B.J. Raney, M.S. Cline, D. Karolchik, G.P. Barber, H. Clawson, et al. 2012. ENCODE whole-genome data in the UCSC Genome Browser: update 2012. *Nucleic Acids Res.* 40:D912–D917. http://dx.doi.org/10.1093/nar/gkr1012

Sabo, P.J., M. Hawrylycz, J.C. Wallace, R. Humbert, M. Yu, A. Shafer, J. Kawamoto, R. Hall, J. Mack, M.O. Dorschner, et al. 2004. Discovery of functional noncoding elements by digital analysis of chromatin structure. *Proc. Natl. Acad. Sci. USA.* 101:16837–16842. http://dx.doi.org/10.1073/pnas.0407387101

Scheinfeldt, L.B., S. Soi, S. Thompson, A. Ranciaro, D. Woldemeskel, W. Beggs, C. Lambert, J.P. Jarvis, D. Abate, G. Belay, and S.A. Tishkoff. 2012. Genetic adaptation to high altitude in the Ethiopian highlands. *Genome Biol.* 13:R1. http://dx.doi.org/10.1186/gb-2012-13-1-r1

Simonson, T.S., Y. Yang, C.D. Huff, H. Yun, G. Qin, D.J. Witherspoon, Z. Bai, F.R. Lorenzo, J. Xing, L.B. Jorde, et al. 2010. Genetic evidence for high-altitude adaptation in Tibet. *Science.* 329:72–75. http://dx.doi.org/10.1126/science.1189406

Stobdan, T., D. Zhou, E. Ao-Ieong, D. Ortiz, R. Ronen, I. Hartley, Z. Gan, A.D. McCulloch, V. Bafna, P. Cabrales, and G.G. Haddad. 2015. Endothelin receptor B, a candidate gene from human studies at high altitude, improves cardiac tolerance to hypoxia in genetically engineered

heterozygote mice. *Proc. Natl. Acad. Sci. USA*. 112:10425–10430. http://dx.doi.org/10.1073/pnas.1507486112

Sturgeon, C.M., A. Ditadi, G. Awong, M. Kennedy, and G. Keller. 2014. Wnt signaling controls the specification of definitive and primitive hematopoiesis from human pluripotent stem cells. *Nat. Biotechnol.* 32:554–561. http://dx.doi.org/10.1038/nbt.2915

Udpa, N., R. Ronen, D. Zhou, J. Liang, T. Stobdan, O. Appenzeller, Y. Yin, Y. Du, L. Guo, R. Cao, et al. 2014. Whole genome sequencing of Ethiopian highlanders reveals conserved hypoxia tolerance genes. *Genome Biol.* 15:R36. http://dx.doi.org/10.1186/gb-2014-15-2-r36

Villafuerte, F.C., J.L. Macarlupú, C. Anza-Ramírez, D. Corrales-Melgar, G. Vizcardo-Galindo, N. Corante, and F. León-Velarde. 2014. Decreased plasma soluble erythropoietin receptor in high-altitude excessive erythrocytosis and Chronic Mountain Sickness. *J. Appl. Physiol.* 117:1356–1362. http://dx.doi.org/10.1152/japplphysiol.00619.2014

Wu, T.Y. 2005. Chronic mountain sickness on the Qinghai-Tibetan plateau. *Chin. Med. J. (Engl.).* 118:161–168.

Xiang, K., Y. Ouzhuluobu, Y. Peng, Z. Yang, X. Zhang, C. Cui, H. Zhang, M. Li, Y. Zhang, Bianba, et al. 2013. Identification of a Tibetan-specific mutation in the hypoxic gene EGLN1 and its contribution to high-altitude adaptation. *Mol. Biol. Evol.* 30:1889–1898. http://dx.doi.org/10.1093/molbev/mst090

Xu, J., H.Y. Sun, F.J. Xiao, H. Wang, Y. Yang, L. Wang, C.J. Gao, Z.K. Guo, C.T. Wu, and L.S. Wang. 2015. SENP1 inhibition induces apoptosis and growth arrest of multiple myeloma cells through modulation of NF-κB signaling. *Biochem. Biophys. Res. Commun.* 460:409–415. http://dx.doi.org/10.1016/j.bbrc.2015.03.047

Yu, L., W. Ji, H. Zhang, M.J. Renda, Y. He, S. Lin, E.C. Cheng, H. Chen, D.S. Krause, and W. Min. 2010. SENP1-mediated GATA1 deSUMOylation is critical for definitive erythropoiesis. *J. Exp. Med.* 207:1183–1195. http://dx.doi.org/10.1084/jem.20092215

Zhao, H.W., X.Q. Gu, T. Chailangkarn, G. Perkins, D. Callacondo, O. Appenzeller, O. Poulsen, D. Zhou, A.R. Muotri, and G.G. Haddad. 2015. Altered iPSC-derived neurons' sodium channel properties in subjects with Monge's disease. *Neuroscience.* 288:187–199. http://dx.doi.org/10.1016/j.neuroscience.2014.12.039

Zhou, D., N. Udpa, R. Ronen, T. Stobdan, J. Liang, O. Appenzeller, H.W. Zhao, Y. Yin, Y. Du, L. Guo, et al. 2013. Whole-genome sequencing uncovers the genetic basis of chronic mountain sickness in Andean highlanders. *Am. J. Hum. Genet.* 93:452–462. http://dx.doi.org/10.1016/j.ajhg.2013.07.011